ARTICLE TYPE

First example of antiparasitic activity influenced by thermochromism: Leishmanicidal evaluation of 5,7-dimethyl-1,2,4-triazolo[1,5-a]pyrimidine metal complexes.

José M. Méndez-Arriaga[a,b]*, Itziar Oyarzabal[c,d], Álvaro Martín-Montes[b], Judith García-Rodríguez[a], Miguel Quirós[a], Manuel Sánchez-Moreno[b]

[a] Department of Inorganic Chemistry, Faculty of Sciences, University of Granada, Avda. Fuentenueva, 18071 Granada, Spain, [b] Department of Parasitology, Faculty of Sciences, University of Granada Avda. Fuentenueva, 18071 Granada, Spain, [c] CNRS, CRPP, UPR 8641, 33600 Pessac, France, [d] University of Bordeaux, CRPP, UPR 8641, 33600 Pessac, France

Abstract: Background: The World Health Organization catalogues illnesses such as Leishmaniasis as neglected diseases, due the low investment in new drugs to fight them. The search of novel and non-side effects anti-parasitic compounds is one of the urgent needs for the Third World. The use of triazolopyrimidines and their metallic complexes have demonstrated hopeful results in this field.

Objective: This work studies the antiparasitic efficacy against three *leishmania spp.* strains of a series of 5,7-dimethyl-1,2,4-triazolo[1,5-a]pyrimidine first row transition metal complexes.

Method: The *in vitro* antiproliferation of promastigote forms of different strains of *leishmania spp.* (*L. infantum*, *L. braziliensis* and *L donovani*) and the cytotoxicity in macrophage host cells are reported here. The antiparasitic assays have been complemented with enzymatic tests to elucidate the mechanisms of action. New crystal structure description, thermal analysis, magnetic susceptibility and magnetization experiments have also been carried out in order to present a whole characterization of the studied compounds and interesting physical properties besides the biological tests.

Results: The results of antiproliferation screening and cytotoxicity show a great antiparasitic efficacy in the studied complexes. The superoxide dismutase enzymatic assays exhibit a different behaviour according to the thermochromic triazolopyrimidine form tested.

Conclusion: Antiproliferative assays and enzymatic tests corroborate the synergetic leishmanicidal effect present in coordination triazolopyrimidine complexes. The changes in coordination sphere derived from thermocromism affect to physical properties as well as biological efficacy.

Keywords: Leishmaniasis, antiparasitic activity, enzymatic inhibition, coordination chemistry, bioinorganic chemistry, magnetism, triazolopyrimidine.

1. INTRODUCTION

According to recent reports of the World Health Organisation (WHO), Leishmaniasis is considered as one of the seven primary illnesses that affects all continents and is broadly located in tropical and subtropical poor regions of the New World, but also present in Europe and Asia by migration[1,2]. About two million new cases arise every year, with an annual mortality rate higher than 60,000 people, a number that is only surpassed by malaria among parasitic diseases[3]. The transmission vectors are mainly dipteral insects that belong to the genera *Phlebotomus* in the Old World and *Lutzomyia* in the New World. Moreover, the recent Syrian refugee crisis has resulted in a catastrophic outbreak of Old World cutaneous leishmaniasis now affecting hundreds of thousands of people living in refugee camps or trapped in conflict zones[4]. This unhealthy situation, related to the blood transfusions from infected patients in host countries, makes Leishmaniasis a global illness that is spreading out on the Third World. Despite of these alarming data, Leishmaniasis is still considered as a neglected disease due to the low investment in the search of new efficient drugs.

In the last five decades, pentavalent antimonials like meglumine antimoniate (Glucantime) and sodium stibogluconate (Pentostam) have been the main treatment against Leishmaniasis. Nevertheless, the molecular structure of antimonials, their metabolism and mechanism of action (MOA) are still being explored[5]. Even though this type of compounds are still the first-line antiparasitic drugs, they exhibit several limitations like severe side effects including vomiting, peripheral polyneuropathy or allergic dermopathy[6], the need of daily parenteral administration and drug resistance[7]. In parallel to this, although in a lesser extent, existing non-antimonial antiparasitic prodrugs as Anfotericine B are also being used as Leishmaniasis treatment[8], but its high price hinders the access and implementation in poor regions, which are the mostly affected areas, and display adverse side effects too, especially kidney failure. Thus, there is an urgent need to find new and more efficient therapies to fight Leishmaniasis, in order to minimize its impact in society.

In this regard, triazolopyrimidine derivatives have proved their notable pharmacology including antipyretic, analgesic, anti-inflammatory, herbicidal, fungicidal, antimicrobial, antitumor and antiparasitic properties[9]. Multiple technological applications have been described for these ligands[10], since their discovery by Bülow and Haas in 1909[11]. In addition, our group has studied the magnetic and luminescent properties of the coordination compounds based on different metal ions with these ligands[12].

Apart from their potential technological application, the growing interest of the scientific community for triazolopyrimidines also comes from their biomimetic character, since they bear a resemblance to the natural occurring purine nucleobases. These bicyclic molecules and some of their metal complexes have shown a great activity against diverse species of *leishmania spp.*[13], making them potential chemotherapeutic agents to combat diseases related to parasites. Several other authors have also pointed out to metal complexes as a promising alternative to fight tropical parasitic diseases caused by members of *Trypanosomatidae* family including the disease under study in this work[14], as well as other tropical illnesses such as Chagas disease or malaria[15]. In all the mentioned cases, a synergetic effect in the antiparasitic efficacy has been observed upon coordination of triazolopyrimidine derivatives to different metal ions[16].

Based on the above findings, and with the design of new drug candidates for potent, selective and less toxic parasitic therapeutic agents as the main target, we have selected 5,7-dimethyl-1,2,4-triazolo[1,5-a]pyrimidine (**dmtp**) to form new antiparasitic metal complexes (**Scheme 1**). Six metal complexes based on **dmtp** derivative are reported herein. Their molecular formulas are $[Cu_2Cl_4(dmtp)_4](H_2O)_2$ **(1)**, in which triazolopyrimidine ligand acts as bridge between both Cu(II) centres, $[Co(dmtp)_2(H_2O)_4]Cl_2(H_2O)_2$ **(2)**, $[Ni(dmtp)_2(H_2O)_4]Cl_2(H_2O)_2$ **(3)**, $[CoCl_2(dmtp)_2]$ **(4)**, $[NiCl_2(dmtp)_2]$ **(5)** and $[Zn(dmtp)_2Cl_2]$ **(6)**. In this regard, we have designed the syntheses of compound **1** and described its structure for the first time; studied the magnetic behaviour of the four most stable complexes; and characterized all of them using thermoanalitical techniques. In addition, *in vitro* anti-proliferative efficacy against extracellular forms of three strains of *Leishmania spp.* (*L. infantum*, *L. braziliensis* and *L. donovani*) has been assayed. Toxicities against macrophage J774.2 host cells have also been determined and the selectivity index (SI) has been compared with values found for the reference Glucantime drugs, free **dmtp** ligand and correspondent inorganic salts, in order to study the

synergetic effect of the complexation in the antiparasitic activity. Finally, their inhibition of parasite Fe-SOD and human CuZn-SOD enzymes has been tested with the aim of elucidating the possible mechanisms of action (MOA) of the assayed compounds.

Scheme 1: Structure of **dmtp** derivative (left, IUPAC ring-numbering system) and adenine (right, biochemical ring-numbering).

2. MATERIALS AND METHOD

All metallic salts and the 5,7-dimethyl-1,2,4-triazolo[1,5-a]pyrimidine (**dmtp**) ligand were purchased from commercial sources and used as received without further purification.

2.1. Preparation of [Cu₂Cl₄(dmtp)₄](H₂O)₂ (1) and [M(dmtp)₂(H₂O)₄]Cl₂(H₂O)₂ where M = Co and Ni (2, 3)

A saturated aqueous solution of $CuCl_2 \cdot 2H_2O$ (1 mmol, 0,170 g) was added to an ethanolic solution containing **dmtp** (2 mmol, 0,296 g) in the minimum volume of solvent, without any heating or stirring. After slow evaporation of the solvent at room temperature for two days, blue crystals suitable for XRD characterization were separated by vacuum filtration.

Anal. Calcd. for $C_{28}N_{16}H_{36}O_2Cu_2Cl_4$: C, 37.47; H, 4.04; N, 24.97. Found: C, 37.22; H, 4.46; N, 24.98%.

An identical synthetic procedure was followed for **2** and **3**, using **dmtp** (2mmol, 0,296g) and the correspondent inorganic salt ($CoCl_2 \cdot 6H_2O$, 1 mmol, 0,238 g and $NiCl_2 \cdot 6H_2O$, 1 mmol, 0,238 g). A different synthetic method through recrystallization of a previous intermediate was recently reported by Marutescu et al. in 2017[17] for complex **2**.

2.2. Preparation of [MCl₂(dmtp)₂] where M = Co, Ni and Zn (4, 5 and 6)

Complexes **4** and **5** were obtained by dehydration of compounds **2** and **3**, respectively, heating at 80 °C for 15 minutes in an oven. The process was irreversible for complex **4**, which changed of colour from orange to dark blue while maintaining the crystallinity, but it was more unstable for complex **5**, as it returned to the hydrated form in less than 24 hours. An alternative direct synthesis was also published by Marutescu et al.[17] for compound **4**. Compound **6** was synthesized following the same procedure as for **1-3**, but in this case there are no crystallization water molecules outside the coordination sphere.

2.3. Physical measurements

Elemental analyses were carried out at the "Centro de Instrumentación Científica" of the University of Granada on a THERMO SCIENTIFIC analyser model Flash 2000. The IR spectra on powdered samples were recorded with a BRUKER TENSOR 27 FT-IR and OPUS data collection program. Thermal behaviour (thermogravimetry – TG – and differential scanning calorimetry – DSC) was studied under an air flow in Shimadzu TGA-50 and Shimadzu DSC-50 equipment at heating rates of 20 and 10 °C min⁻¹, respectively. Variable-temperature (2-300 K) magnetic susceptibility and magnetization measurements at different fields (0-50000 Oe) on polycrystalline samples were carried out with a Quantum Design SQUID MPMS XL5 magnetometer for compounds **1-4**. Diamagnetic corrections were estimated from the Pascal's constants.

2.4. Single-crystal structure determination

A prismatic crystal of **1** was mounted on a glass fibre and used for data collection on a Bruker Smart diffractometer equipped with an APEX detector and graphite monochromated *MoKα* radiation (λ=0.71073Å). The data reduction was performed with the APEX2[18] software and they were corrected for absorption using SADABS[19]. The structure was solved by direct methods and anisotropically refined by full-matrix least-squares on F^2 by means of the SHELX-14 program package[20]. Suitable DRX quality crystals of complex **2** were isolated and measured by our research group, but its crystallographic data were recently reported by Marutescu et al. in 2017[17]. Powder diffraction experiment on this compound were registered on a Bruker D2 PHASER equipment (radiation λ=1.54184 Å), showing that it is isostructural with the nickel compound (Complex **3**, **Figure S1**). XRD suitable crystals of **4** and **6** were not obtained, but the crystallographic data has been also published[21,22].

2.5. Parasite strain, culture

Promastigote forms of *L. infantum* (MCAN/ES/2001/UCM-10), *L. braziliensis* (MHOM/BR/1975/M2904) and *L. donovani* (LCRL133LRC) were cultivated in vitro in trypanosomal liquid medium (MTL) [Hank's Balanced Salt Solution-HBSS (Gibco), $NaHCO_3$, lactalbumin, yeast extract, bovine hemoglobin and antibiotics] with 10% inactive fetal bovine serum and were kept in an air atmosphere at 28 °C, in Roux flasks (Corning, USA) with a surface area of 75 cm², according to the methodology described by Gonzalez et al.[23]. The screening of extracellular forms of parasites were carried out by using 24-well plates with MTL medium and 5×10^4 parasites per well. The products were tested at 1, 10, 25 and 50 µM, leaving some wells without drugs as control, and were incubated at 28 °C during 72 hours before the parasite final count.

2.6. Cell culture and cytotoxicity test

J774.2 macrophages (European Collection of Cell Culture – ECACC – number 91051511), which were originally obtained from a tumour in a female BALB/c rat in 1968, were grown in minimum essential medium (MEM) containing glutamine (2mM) and supplemented with 20% inactivated fetal bovine serum. The incubation of the cells was carried out using a humidified 95% air, 5% CO_2 atmosphere at 37°C for several days. The cytotoxicity tests for host cells were performed in 96-well plates that serve to measure in the ELISA reader and the products were tested at 50, 100, 200 and 400 µM. First, the cells were sowed in a 96-well plate (2500 cells / well) to a volume of 100 µL / well and then were incubated at 37 °C with 5% CO_2 during 24h. The different complexes solutions were prepared in advance at the double of the highest concentration to be tested in culture medium (MEM+Glut 20% SBF). The solutions were performed in a sterile bath with the different channels, by adding 100 µL of complex solution or medium (only adding medium in the control wells) to the corresponding well. After that, the plate was incubated at 37 °C with 5% CO_2 for 48 hours. Two days after, 20 µL of Alamar Blue dye (10% of the volume of the well) were added to each well and they were incubated at 37 °C with 5% CO_2 during one day more. The whole incubation time once the products were added was 72 hours, coinciding with the screening period to have comparable selectivity index results. Finally, the plate was read with reader in ELISAs with Alamar Blue and the data were mathematically treated using linear regression analysis from the K_c values of the concentrations employed to obtain IC_{50} inhibition values.

2.7. Fe-SOD and CuZn-SOD enzymatic inhibition

Parasites were collected in the logarithmic growth phase by centrifugation (400 g for 10 min at room temperature). After centrifugation, the obtained pellet was suspended in 3 mL of STE buffer (0.25 M sucrose, 25 mM Tris–HCl, 1 mM EDTA, pH= 7.8) and the cells were lysed by three cycles of sonication for 30 s each at 60 W. The sonicated homogenate was centrifuged at 1500 g for 5 min at 4 °C, and the pellet was washed three times in ice-cold STE buffer. This fraction was centrifuged (2500 g for 10 min at 4 °C) and the supernatant was collected. After that, the supernatant was subjected to ice-cold ammonium sulphate precipitation between 35 and 85% salt concentration and the resulting precipitate was dissolved in 2.5 mL of distilled water and desalted by chromatography in Sephadex G-25 column (GE Healthcare Life Sciences®, PD 10 column) previously equilibrated with 2 mL of distilled water, taking it up to a final volume of 3.5 mL. The content of protein Fe-SOD was quantified by using the Sigma Bradford test, which uses BSA as a standard[24]. The activity of iron superoxide dismutase was determined using a previously described method[25], which measures the reduction in nitroblue tetrazolium (NBT) by superoxide ions. Following the protocol, 845 µL of stock solution [3 mL of L-methionine (300 mg, 10 mL^{-1}), 2 mL of NBT (1.41 mg, 10 mL^{-1}) and 1.5 mL of Triton X-100 1% (v/v)] were added into each well, together with 30 µL of the parasite homogenate fraction, 10 µL of riboflavin (0.44 mg, 10 mL^{-1}), and an equivalent volume of the different concentrations of the compounds that were tested. Different concentrations were used for each agent, from 0 to 100 µM. In the control experiment the volume was increased to 1000 µL with 50 mM potassium phosphate buffer (pH = 7.8, 3 mL), and 30 µL of the parasite homogenate fraction added to the mixtures containing the compounds. First, the absorbance (A0) was measured at 560 nm in a UV spectrophotometer. Afterwards, each well was illuminated with UV light for 10 min under constant stirring and the absorbance (A1) was measured again. The human CuZn-SOD and substrates used in these assays were obtained from Sigma Chemical Co. The resulting data were analysed using the Newman-Keuls test.

3. RESULTS

3.1. Crystal structures
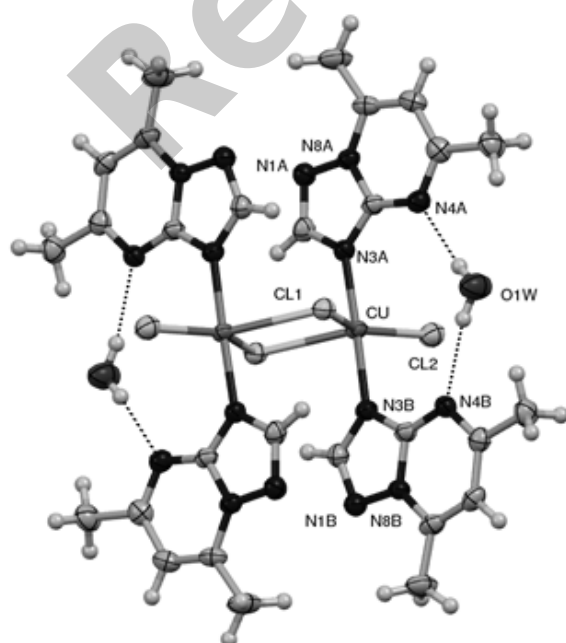
3.1.1. Crystal structure of [Cu$_2$Cl$_4$(dmtp)$_4$](H$_2$O)$_2$ (1)

Complex **1** crystallizes in the triclinic P-*1* space group. X-ray crystal structure of **1** is displayed in **Figure 1**. Selected bond lengths and angles are given in **Table S1**. Final R(F), wR(F^2) and goodness of fit agreement factors, details on the data collection and analysis can be found in **Table S2**. The crystallographic data have been deposited at the Crystallography Open Database and are freely downloadable at the URL www.crystallography.net/3000200.html. They have also been deposited at the Cambridge Crystallographic Data Centre (deposition number 1843310) and can be obtained free of charge via www.ccdc.cam.ac.uk/data_request/cif.

Figure 1: Perspective view of [Cu$_2$Cl$_4$(dmtp)$_4$](H$_2$O)$_2$ **(1).**

The structure consists of dinuclear [Cu$_2$Cl$_4$(dmtp)$_4$] entities, with two crystallization water molecules stabilizing the crystal structure. The copper ions are linked to each other by chlorine bridging ligands, leading to a four membered ring. Each metallic centre possesses a distorted trigonal bipyramid geometry, the equatorial positions are filled with the chlorine atoms while the **dmtp** ligands are coordinated in a N3 monodentate mode in the axial positions. As expected, the Cu-X (X = Cl or N) bond distances are shorter for the axially located ligands (Cu-N3A=1.9997 Å, Cu-N3B=2.005 Å, Cu-Cl1=2.3993 Å and Cu-Cl2=2.2831 Å). The four chlorine atoms are coplanar with the two copper centres. The bond angles are N3A-Cu-N3B=177.82 °, N3-Cu-Cl=90.03-90.64 ° and Cl2-Cu-Cl1=146.16 °. Finally, both crystallization water molecules interact with two different **dmtp** ligands by N4 atoms mediated hydrogen bonds, stabilizing this way the whole structure. An isostructural structure, including bromine bridging atoms instead of chlorine atoms, was described by our group previously[21].

3.1.2. Crystal structure of [Co(dmtp)$_2$(H$_2$O)$_4$]Cl$_2$(H$_2$O)$_2$ (2)

The second type of triazolopyrimidine complexes studied in this work (**2** and **3**, whose isostructuralism is confirmed by x-ray powder, **Figure S1**) crystallizes in the triclinic P-*1* space group. The main structure of compound **2** is comprised of a cobalt cationic complex [Co(dmtp)$_2$(H$_2$O)$_4$]$^{2+}$, two interstitial water molecules and two chloride anions that balance the charge. The metal ion is located in the inversion centre of the centrosymmetric cationic unit and it exhibits an octahedral CoN$_4$O$_2$ environment due to coordination to two water molecules and four different dmtp ligands. The structure was previously published[17], as well as an isostructural compound was also published by our group two decades ago[22].

3.1.3. Crystal structure of [M(dmtp)$_2$(Cl)$_2$] where M = Co, Ni and Zn (4, 5 and 6)

Complex **4** crystallizes in the orthorhombic *P*bca space group. In this case, the cobalt centre adopts a tetrahedral CoN$_2$Cl$_2$ coordination geometry due to the linkage to two chloride anions and two triazolopyrimidine molecules through the N3 atom. Full structural description can be found in L. Marutescu et al.[17]. Compound **6**, described by J.M.

Salas et al.[26], is isostructural with **4**, as well as with the nickel containing compound (**5**).

3.2. Spectroscopic properties

The 1700–1500 cm^{-1} region of the infrared spectrum of the dmtp ligand displays two characteristic bands, one of which is assigned to the vibration mode of the triazolopyrimidinic skeleton (1638 cm^{-1}), while the other one comes from the vibration of the pyrimidinic ring (1548 cm^{-1}). Both are slightly affected by the metal coordination. A broad band belonging to the crystallization water molecules is present in the zone of 3000-3500 cm^{-1} in hydrated complexes (spectrum of complex **1** is in **Figure S2**, the rest can be found in bibliography).

3.3. Thermal behaviour

Even though some of the complexes presented in this work have already been physical and spectroscopically characterized, their thermoanalitical study is exposed here for first time. The first stage in the thermogravimetric curve of compound **1** is a one-step dehydration process, starting at 160 °C. The dehalogenation process starts at 270 °C and is followed by a pyrolitic decomposition of **dmtp** ligands, leaving CuO as final residue (**Figure S3**). Complexes **2** and **3** exhibit a similar pattern to that of **1**, with one-step dehydration processes starting at lower temperatures (88 and 98 °C, respectively) that continue with dehalogenation processes at 269 and 258 °C, respectively. In the case of dehydrated compounds **4**-**6**, the thermoanalitical curves are simpler, and are composed of intense and endothermic dehalogenation processes that are followed by endothermal decomposition of the triazolopyrimidine ligands in a short range of high temperatures (230-260 °C for dehalogenation, 320-340 °C for ligand decomposition). **Figure S4** in electronic supporting information illustrates the evolution of the sample analysis for complex **4**. **Table S3** shows theoretical and experimental dehydration and oxide residues of the six **dmtp** complexes (**1-6**).

3.4. Magnetic properties

In order to complete the characterization of these **dmtp** complexes, studies of magnetic susceptibility and magnetization have been carried out. The temperature dependence of the $\chi_M T$ product (χ_M being the molar paramagnetic susceptibility of the compounds) under a constant magnetic field of 0.1 T and the field dependence of the magnetization at 2 K for compound **1** is inserted in the text (**Figure 2**), while the rest are displayed in **Figures S5-S8**. Instability of complex **5** and diamagnetism of complex **6** excluded them from these assays.

Starting with complex **1** ([Cu$_2$Cl$_4$(dmtp)$_4$](H$_2$O)$_2$), the room temperature $\chi_M T$ value of 0.85 cm^3 K mol^{-1} is consistent with the expected value for two non-interacting Cu(II) ions (S = 1/2) with g = 2.0 (0.75 cm^3 K mol^{-1}). The $\chi_M T$ value remains almost constant until ~50 K and then drops abruptly reaching a value of 0.07 cm^3 K mol^{-1} at 2 K. This magnetic behaviour indicates the occurrence of antiferromagnetic (AF) exchange interactions within the Cu(II) dinuclear units, together with intermolecular interactions. In keeping with this, the thermal variation of the χ_M shows a maximum at 5 K (**Figure S5**). The magnetic

susceptibility data was modelled using the following Hamiltonian:

$$H = -JS_{Cu}S_{Cu} - zJ'<S_z>S_z + g_e\mu_B SH$$

where *J* is the magnetic exchange pathway through the dichloro double bridge, $-zJ' < S_z > S_z$ accounts for the intermolecular interactions by means of the molecular field approximation, g_e is the average *g* factor, μ_B is the Bohr magneton and *H* is the magnetic field. The best fit using the full-matrix diagonalization PHI program[27] afforded the following set of parameters: *J* = -5.14 cm^{-1}, *zJ* = -0.34 cm^{-1} and g_e = 2.14 with *R* = 6.7·10^{-5} (R = $\Sigma[(\chi_M T)_{exp.} - (\chi_M T)_{calcd.}]^2/\Sigma((\chi_M T)_{exp})^2$). The obtained parameters agree well with the values found for other halide bridged dinuclear Cu(II) complexes[28]. On the other hand, magnetization experiments show a progressive magnetization increase as the applied magnetic field increases without reaching the expected saturation value for a S = 1 ground state at fields as high as 50000 Oe, which is consistent with the weak AF interactions observed in this compound.
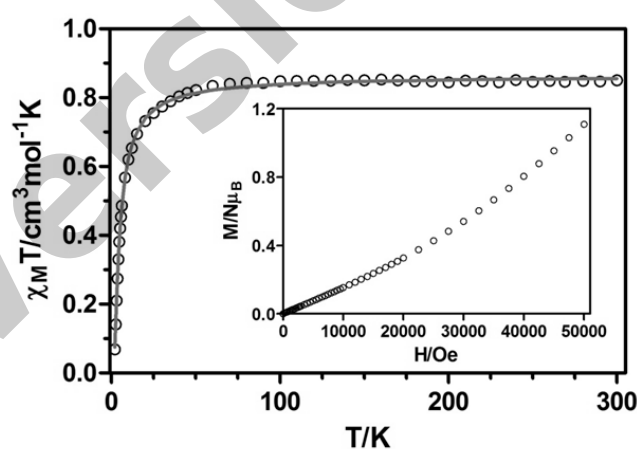

Figure 2: Temperature dependence of $\chi_M T$ for **1**. The solid line represents the best fit to the Hamiltonian indicated in the text. Inset: field dependence of the magnetization for **1**.

Regarding complex **2** ([Co(dmtp)$_2$(H$_2$O)$_4$]Cl$_2$(H$_2$O)$_2$), the $\chi_M T$ value of 2.54 cm^3 K mol^{-1} at room temperature is larger than the spin-only value for high-spin Co(II) ions (S = 3/2, 1.875 cm^3 K mol^{-1}), which is due to the significant contribution of the orbital angular momentum to the ground state (**Figure S6**) [21,29]. On lowering the temperature, $\chi_M T$ remains practically constant in the high temperature range and it decreases sharply below 120 K, reaching a value of 1.47 cm^3 K mol^{-1} at 2 K. The observed behaviour points towards spin-orbit coupling (SOC) effects, although it could also be due to intermolecular AF interactions. Since the magnetic interactions between individual metallic centres are usually weak enough to be masked by the SOC effects of the Co(II) ions, the susceptibility data were fitted to the following Hamiltonian:

$$H = D [S_z^2 - S(S+1)/3] + g_e\mu_B SH$$

where *D* accounts for the axial magnetic anisotropy, *S* is the spin of the ground state and the rest of the terms have the same meaning as in the above mentioned Hamiltonian. The best fitting parameters were *D* = |40.8| cm^{-1} and g_e = 2.34, which are

consistent with the values found in bibliography for other octahedral Co(II) ions[30]. It should be noted that the sign of D could not be unambiguously determined from the $\chi_M T$ data, which is common for S = 3/2 systems.

The $\chi_M T$ value for complex **3** ($[Ni(dmtp)_2(H_2O)_4]Cl_2(H_2O)_2$) at room temperature is of 1.29 cm³ K mol⁻¹, which is slightly higher but in good agreement with the expected value for a Ni(II) ion (S = 1) with g = 2.0 (1.0 cm³ K mol⁻¹) (**Figure S7**). On cooling, the $\chi_M T$ product remains almost constant until 20 K, and then drops abruptly to reach a value of 0.76 cm³ K mol⁻¹ at 2 K. This behaviour suggests the existence of zero field splitting effects, which are promoted by the local anisotropy of the Ni(II) ions. In addition, the magnetization curve at 2 K shows a gradual increase with the applied field without reaching a complete saturation at 50000 Oe, thus corroborating the presence of significant anisotropy.

After dehydration, the $\chi_M T$ product at high temperatures of the Co compound shows a similar trend to that of complex **2**, indicating that the SOC effects are also present in compound **4** ($[CoCl_2(dmtp)_2]$) (**Figure S8**). However, the $\chi_M T$ product of complex **4** starts decreasing at lower temperatures (around 50 K), displaying a value of 1.65 cm³ K mol⁻¹ at 2 K. As expected, the fit of the susceptibility data to the above Hamiltonian led to a lower anisotropy parameter (D = |8.98| cm⁻¹), while there were no significant changes in the average *g* factor (g_e = 2.33). The obtained values are in good agreement with those found for pseudotetrahedral Co complexes of the type $[CoN_2Cl_2]$ [31]. The *M* vs. *H* plots at 2 K for both Co(II) complexes show similar behaviour, where the magnetization is not fully saturated even at an applied field of 50000Oe. The *M* values of 2.30 and 2.49 μ_B obtained at 5 T respectively for **2** and **4** are lower than the expected value of 3 μ_B, which is due to anisotropy.

3.5. *In vitro* Antiparasitic Activity and Toxicity of dmtp complexes (1-5)

Actual treatments against *Leishmaniasis*[32] usually present toxicity problems, limited efficacy and resistance by some parasite strains. All of these disadvantages make it necessary to explore other possibilities for improved therapies and new drug development. Taking into account the encouraging properties of the metallic complexes with triazolopyrimidine ligands, we decided to check the mentioned complexes against three strains of *leishmania spp.* and to compare them with the commercial drug Glucantime, isolated **dmtp** derivative and correspondent inorganic salts (**Table S3**). The instability of complex **5** excluded it from these assays.

The Ni(II) complex (**3**) displays the best antiproliferative activity against promastigote growth in the three assayed strains, with an extraordinary 46 fold higher SI than the reference drug Glucantime in the case of *L. infantum*, and with great values also for the other two strains. The excellent intracellular form antiproliferetive results are accompanied with a very low toxicity for the host human cells, which means a high efficacy against parasite with an innocuous effect in the patient. Complex **1** shows a moderate efficacy against *leishmania spp.*, but it is only clearly superior to the reference drug and free **dmtp** ligand for *L. infantum*. The cobalt complexes (**2 and 4**) exhibit a similar range of good antiproliferative SI coefficients,

but with differences on the antiparasitic activity depending on the thermochromic form or the strain analysed, remarking that both complexes probably interact in a different mode with the parasites. Finally, the zinc complex has the lowest activity against promastigote forms, exhibiting a practically identical behaviour to that of the reference drug Glucantime in most cases. The behaviour of complex **6** is in good agreement with previous studies with triazolopyrimidine compounds[15c]. As expected, no inhibition activity was obtained for the free inorganic salts. These results uphold the synergetic effect observed in previous studies of triazolopyrimidine complexes against *leishmania spp.*[15] The results are shown in **Figure 3**.
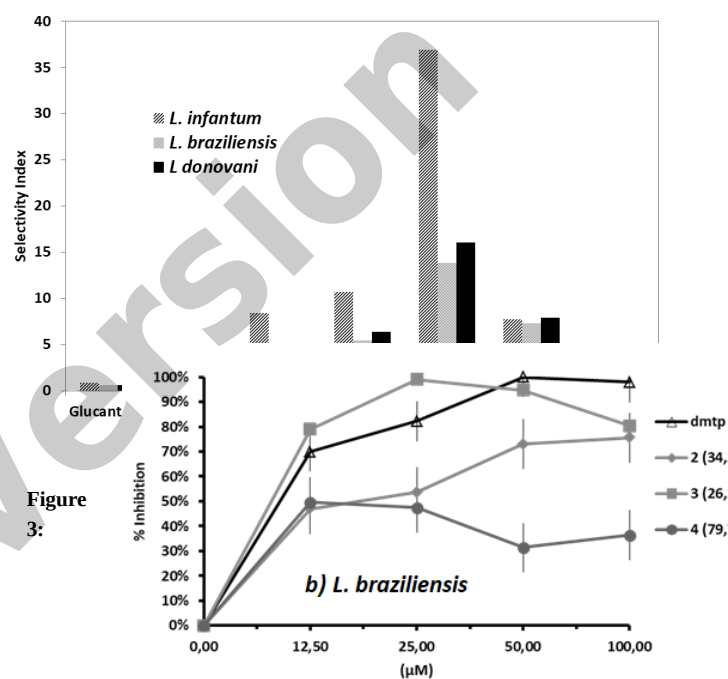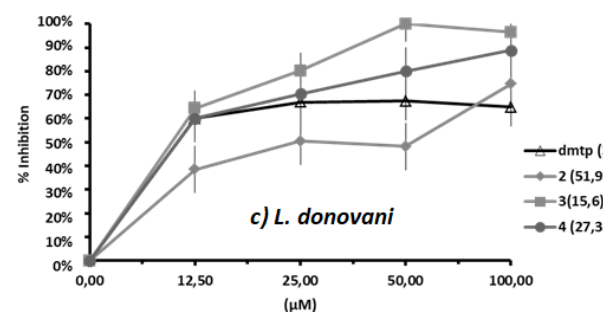

Figure 3:

Comparative SI values between reference drugs, free dmtp ligand and complexes **1-4** and **6**.

3.6. Activity against SOD

The identification of drug targets is imperative to develop new effective drugs against Leishmaniasis[33], so the study of the inhibition of antioxidant enzymes capable of preventing

oxidative stress are in the spotlight. Within this group, a basic defence mechanism against oxidation in parasites is provided by the iron superoxide dismutase (Fe-SOD) enzyme, which is located in the cytosol, the mitochondria and the glycosomes and

plays an important role in the transformation of harmful superoxide radicals into oxygen and hydrogen peroxide[34]. Consequently, molecules that are able to inhibit selectively the Fe-SOD could be promising candidates as leishmanicidal agents[14d,35]. Since prosthetic groups are essential in all processes regulated by the enzyme, alterations in the active centre of these molecules could effectively leave without effect its antioxidant activity and thus influence both the growth and survival of the parasite cells[14c]. The mentioned deactivation can be induced by modifications in the coordination geometry or by dissociation of the iron atom. In addition, a complementary advantage of using Fe-SOD as a drug target resides in their absence in human biological systems, which use CuZn-SOD and Mn-SOD for the same purpose. This way, we can eliminate an undesired effect on the enzymatic human system by a selective inhibition of Fe-SOD.

The highly promising results reached in the *in vitro* studies for complex **3** prompted us to study this relevant mechanistic mode of antiparasitic action. Both forms of the Co complex (**2** and **4**) were also evaluated, in order to elucidate the relevant structural parameters derived from thermocromism for an optimal antiproliferative action against promastigote forms. We tested the effects of **dmtp** and the three complexes on Fe-SOD isolated from *L. infantum, L. braziliensis* and *L. donovani* over a wide range of concentrations (from 0 to 100 μM). The obtained inhibition data are shown in **Figure 4a-c**, and the corresponding IC_{50} values are indicated in brackets to clarify the interpretation of the results. The most remarkable result is that **dmtp** only inhibits Fe-SOD activity significantly in the case of *L. braziliensis*, while the complexes exhibit a variety of inhibitions depending on the strain and metal centre. These results confirm that the triazolopyrimidine complexes with **dmtp** show specific antiparasitic activity, and there is a synergetic effect between the coordinated ligand and the metal centre.
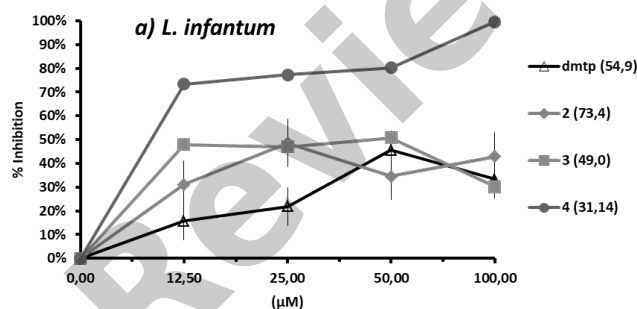

Figure 4: In vitro inhibition (%) of Fe-SOD in (a) *L. infantum*, b) *L. braziliensis* and c) *L. donovani* promastigotes for studied compounds. Differences between the activities of the control homogenate and those incubated with the **dmtp** and **2-4** were analysed with the Newman–Keuls test. IC_{50} (in brackets) was calculated by linear regression analysis from the Kc values at the employed concentrations (0, 12.5, 25, 50 and 100 μM).

As it can be noticed in **Figure 4**, the three assayed complexes exhibit better inhibition percentage than the free ligand **dmtp**, with the exception of *L. braziliensis* where the antiparasitic enzymatic activity is only surpassed by the nickel compound (**3**) at low concentrations. Complex **3** exhibits consistent inhibition

values in the three assayed strains. On the other hand, both thermochromic cobalt complexes show different inhibition ratio depending on the type of parasite strain. The dehydrated cobalt complex (**4**) possesses an inhibition percentage close to 100% at high concentrations against *L. infantum*, while the hydrated form (**2**) displays similar behaviour to that of the **dmtp** ligand (**Figure 4a**). The opposite trend is observed in **Figure 4b**, where **2** is a more effective prodrug than **4**. This behaviour is in good agreement with the hypothesis that modifications on the structure of similar complexes or variations in the coordination sphere lead to different mechanisms of enzymatic action.

In order to discard possible interferences between parasitic and human SOD enzymes in a potential treatment, the three complexes were also assayed against CuZn-SOD, showing lower inhibition ratios in all the cases. These results confirm specificity of triazolopyrimidine complexes against parasite enzyme instead of human enzyme, making these molecules useful as agents against Fe-SOD target with low interferences with human analogue enzymes. The results are represented in **Figure 5**.

Figure 5: *In vitro* inhibition (%) of human CuZn-SOD for studied compounds. Values are means of separate determinations. Differences between the activities of the control homogenate and those incubated with the **2-4** complexes were analysed with the Newman–Keuls test. IC_{50} (in brackets) was calculated by linear regression analysis from the Kc values at the concentrations employed (0, 12.5, 25, 50 and 100 μM).

To the best of author's knowledge, this manuscript describes the first study of these **dmtp** complexes and the mode of interactions of the antiparasitic compounds with respect to parasite Fe-SOD and human CuZn-SOD enzymes. It is the first enzymatic study which correlates thermochromic forms of a complex with different antiparasitic activity, opening up a refreshing approach to bioinorganic antiparasitic prodrugs development.

CONCLUSION

Six triazolopyrimidine complexes have been studied in this work. Crystal structure of the novel triazolopyrimidine complex $[Cu_2Cl_4(dmtp)_4](H_2O)_2$ (**1**) is reported and the compounds are thermally and magnetically analysed. The antiparasitic efficacy of five of these complexes are assayed, finding a great antiproliferative activity against promastigote forms of parasite, especially in the ni analogue, making it a promising candidate for further *in vivo* experiments. Moreover, parasite Fe-SOD and human cuzn-sod enzyme inhibition tests are carried out, in the search of mechanisms of action (moa). Different enzymatic inhibition effect is observed for the thermocromic co complex forms, illustrating the importance of structural changes and variations in the coordination sphere in the antiparasitic activity. Both antiproliferative assays and sod tests corroborate the synergetic effect present in coordination triazolopyrimidine complexes with antiparasitic activity.

HUMAN AND ANIMAL RIGHTS

No Animals/Humans were used for studies that are base of this research.

CONFLICT OF INTEREST

The authors declare no conflict of interest, financial or otherwise.

SUPPLEMENTARY MATERIAL

Supporting electronic information and crystallographic data are provided.

REFERENCES

[1] Alvar, J., Vélez, I.D., Bern, C., Herrero, M., Desjeux, P., Cano, J., Jannin, J., den Boer, M., WHO Leishmaniasis Control Team, *PLoS One*, **2012**, *7*, e35671.

[2] World Health Organization, Control of the Leishmaniases, report of a WHO expert committee. *World Health Organ Tech Rep Ser.,* **2010**, *949*, 1–186.

[3] Hotez, P.J., Molyneux, D.H., Fenwick, A., Kumaresan, J., Sachs, S.E., Sachs, J.D., Savioli, L., *N. Engl. J. Med.,* **2007**, *357*, 1018-1027.

[4] Du, R., Hotez, P.J., Al-Salem, W.S., Acosta-Serrano, A., *PLoS Negl. Trop. Dis.*, **2016**, 10(5)

[5] Mishra J., Saxena A., *Curr. Med. Chem.*, **2007**, *14*, 1153–1169.

[6] a) Momeni, A.Z., Reiszadae, M.R., Aminjavaheri, R., *Int. J. Dermatol.,* **2002**, *41*, 441–443. b) E. Palumbo, *Am. J. Ther.,* **2009**, *16*, 178–182.

[7] a) Croft, S.L., Sundar, S., Fairlamb, A.H., *Clin. Microbiol. Rev.,* **2006**, *19*, 111–126. b) Natera, S., Machuca, C., Padrón-Nieves, M., Romero, A., Díaz, E., Ponte-Sucre, A., *Int. J. Antimicrob. Agents*, **2007**, *29*, 637–642.

[8] Frézard, F., Demicheli, C., Ribeiro, R.R., *Molecules,* **2009**, *14*, 2317–2336.

[9] a) Salas, J.M., Romero, M.A., Sánchez. M.P., Quirós, M., *Coord. Chem. Rev.,* **1999**, *195*, 1119-1142. b) Magán, R., Marín, C., Rosales, M.J., Barrera, M.A., Salas, J.M., Sánchez-Moreno, M., *Pharmacology*, **2004**, *70*, 83–90. c)

Fischer, G., *Adv. Heterocycl. Chem.*, **2008**, *95,* 143-219. d) Astakhov, A.V., Sokolov, A.N., Pyatakov, D.A., Shishkina, S.V., Shishkin, O.V., Chernyshev, V.M., *Chem. Heterocycl. Comp.*, **2016,** *51,* 1039–1047. e) Botros, S., Khamil, O.M., Kamel, M.M., El-Dash, Y.S., *Acta Chim. Slov,.* **2017**, *64(1)*, 102-116. f) Wang, S., Zhao, L.J., Zheng, Y.C., Shen, D.D., Miao, E.F., Qiao, X.P., Zhao, L.J., Liu, Y., Huang, R.L., Yu, B., Liu, H.M., *Eur. J. Med. Chem.*, **2017,** *125*, 940-951.

[10] Birr, E.J., *Wiss. Z. Phot.*, **1952**, *47*, 2–27.

[11] Bulow, C., Haas, K., *Chem. Ber.*, **1909**, *42*, 4638–4644.

[12] a) Caballero, A.B., Rodríguez-Diéguez, A., Vidal, I., Dobado, J.A., Castillo, O., Lezama, L., Salas, J.M., *Dalton Trans.*, **2012**, *41(6)*, 1755–1764. b) Méndez-Arriaga, J.M., Oyarzabal, I., Escolano, G., Rodríguez-Diéguez, A., Sánchez-Moreno, M., Salas, J.M., *J. Inorg. Biochem.,* **2018**, *180*, 26-32.

[13] a) Caballero, A.B., Rodríguez-Diéguez, A., Quirós, M., Lezama, L. Salas, J.M., *Inorg Chim Acta*, **2011,** *378(1),* 194–201. b) Méndez-Arriaga, J.M., Esteban-Parra, G.M., Juárez, M.J., Rodríguez-Diéguez, A., Sánchez-Moreno, M., Salas, J.M., *J. Inorg. Biochem.*, **2017**, *175*, 217-224.

[14] a) Magán, R., Marín, C., Rosales, M.J., Salas, J.M., Sánchez-Moreno, M., *Pharmacology,* **2005**, *73*, 41–48. b) Martinez, A., Carreon, T., Iniguez, E., Anzellotti, A., Sanchez, A., Tyan, M., Sattler, A., Herrera, L., Maldonado, R.A., Sanchez-Delgado, R.A., *J. Med. Chem.*, **2012**, *55*, 3867-3877. c) Navarro, P., Sanchez-Moreno, M., Marín, C., García-España, E., Ramírez-Macías, I., Olmo, F., Rosales, M.J., Gómez-Contreras, C., Yunta, M.J.R., Gutierrez-Sanchez, R., *Parasitology,* **2014**, *141*, 1031–1043. d) Fandzloch, M., Méndez-Arriaga, J.M., Sánchez-Moreno, M., Wojtczak, A., Jezierska, J., Sitkowski, J., Wisniewska, J., Salas, J.M., Łakomska, I., *J. Inorg. Biochem.*, **2017**, *176*, 144-155.

[15] a) Sánchez-Delgado, R.A., Anzellotti, A., *Mini Rev. Med. Chem.*, **2004**, *4(1),* 23-30. b) Łakomska, I., Fandzloch, M., *Coord. Chem. Rev.*, **2016**, *328*, 221–241. c) Salas, J.M., Caballero, A.B., Esteban-Parra, G.M., Méndez-Arriaga, J.M., *Curr. Med. Chem.,* **2017**, *24(25)*, 2796-2806.

[16] a) Łakomska, I., Fandzloch, M., Wojtczak, A., *Inorg. Chem. Comm.*, **2014**, *49*, 24–26. b) Caballero, A.B., Rodríguez-Diéguez, A., Quirós, M., Salas, J.M., Huertas, O., Ramírez-Macías, I., Sánchez-Moreno, M., *Eur. J. Med. Chem.*, **2014**, *85*, 526–534. c) Guiset-Miserachs, H., Cipriani, M., Grau, J., Vilaseca, M., Lorenzo, J., Medeiros, A., Comini, M., Gambino, D., Otero, L., Moreno, V., *J. Inorg. Biochem.,* **2015**, *150,* 38-47. d) Rodríguez-Arce, E., Machado, I., Rodríguez, B., Lapier, M., Zúñiga, M.C., Maya, J.D., Olea-Azar, C., Otero, L., Gambino, D., *J. Inorg. Biochem.,* **2017**, *170*, 125-133.

[17] Marutescu, L., Calu, M., Chifiriuc, C., Bleotu, C., Daniliuc, C.G., Falcescu, D., Kamerzan, C.M., Badea, M., Olar, R., *Molecules,* **2017**, *22*, 1233.

[18] Bruker Apex2, Bruker AXS Inc., **2004**, Madison, Wisconsin, USA.

[19] Sheldrick, G.M., SADABS, Program for Empirical Adsorption Correction, **1996**, Institute for Inorganic Chemistry, University of Gottingen, Germany.
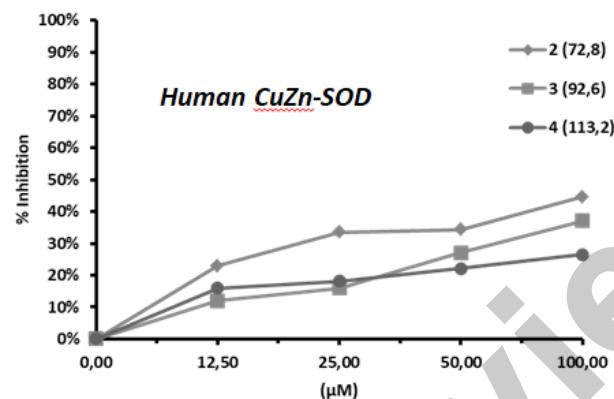
[20] Sheldrick, G.M., **2015**, Acta Cryst. C71, 3-8.

[21] Romero, M.A., Salas, J.M., Quirós, M., Sánchez, M.P., Romero, J., Martín, D., *Inorg. Chem.*, **1994**, *33,* 5477-5481

[22] Romero, M.A., Salas, J.M., Quirós, M., *Transition Met. Chem.,* **1993**, *18*, 595-598.

[23] González, P., Marín, C., Rodríguez-González, I., Hitos, A.B., Rosales, M.J., Reina, M., Díaz, J.G., González-Coloma, A., Sánchez-Moreno, M., *Int. J. Antimicrob. Agents*, **2005**, *25*, 136–141.

[24] Bradford, M.M., *Anal. Biochem.*, **1976**, *72*, 248–254.

[25] Beyer, W.F., Fridovich, I., *Anal. Biochem.,* **1987**, *161*, 559–566.

[26] Salas, J.M., Romero, M.A., Rahmani, A., Faure, R., *Acta Cryst.* 1994, *C50,* 510–512.

[27] Chilton, N.F., Anderson, R.P., Turner, L.D., Soncini, A., Murray, K.S., *I. Comput. Chem.*, **2013**, *34*, 1164-1175.

[28] a) Rojo, T., Arriortua, N.I., Ruiz, J., Darriet, J., Villeneuve, G., Beltran-Porter, D., *Dalton Trans.*, **1987**, 285-291. b) Torres-García, P., Luna-Giles, F., Bernalte-García, A., Platas-Iglesias, C., Esteban-Gómez, D., Viñuelas-Zahínos, E., *New J. Chem.*, **2017**, 41, 8818-8827.

[29] a) Boča, R., *Coord. Chem. Rev.,* **2004**, *248,* 757-815, and references cited therein. b) Titiš, J., Boča, R., *Inorg. Chem.*, **2011**, *50,* 11838-11845.

[30] a) Colacio, E., Ruiz, J., Ruiz, E., Cremades, E., Krzystek, J., Carretta, S., Cano, J., Guidi, T., Wernsdorfer, W., Brechin, E.K., *Angew. Chem. Int. Ed.,* **2013**, *52,* 9130-9134. b) Herchel, R., Vahovska, L., Potočňak, I., Travniček, Z., *Inorg. Chem.*, **2014**, *53*, 5896-5898.

[31] a) Smolko, L., Černák, J., Dušek, M., Miklovič, J., Titiš, J., Boča, R., *Dalton Trans.,* **2015**, *44,* 17565-17571. b) Idešicová, M., Titiš, J., Krzystek, J., Bocǎ, R., *Inorg. Chem.,* **2013**, *52,* 9409-9417.

[32] Caballero, A.B., Salas, J.M., Sánchez-Moreno, M., Metal Based Therapeutics for Leishmaniasis. In Leishmaniasis – Trends in Epidemiology, Diagnosis and Treatment, in *Leishmaniasis: Trends in Epidemiology, Diagnosis and Treatment*, David M. Claborn, Ed. IntechOpen, **2014,** Chapter 20

[33] a) Tavares, J., Ouaissi, A., Kong Thoo Lin, P., Loureiro, I., Kaur, S., Roy, N., Cordeiro-da-Silva, A., *ChemMedChem*, **2010**, *5,* 140-147. b) Cleghorn, L.A., Woodland, A., Collie, I.T., Torrie, L.S., Norcross, N., Luksch, T., Mpamhanga, C., Walker, R.G., Mottram, J.C., Brenk, R., Frearson, J.A., Gilbert, I.H., Wyatt, P.G., *ChemMedChem*, **2011,** *6,* 2214-2224. c) Toro, M.A., Sánchez-Murcia, P.A., Moreno, D., Ruiz-Santaquiteria, M., Alzate, J.F., Negri, A., Camarasa, M.J., Gago, F., Velázquez, S., Jiménez-Ruiz, A., *ChemBioChem*, **2013**, *14(10)*, 1212-7. d) Ruiz-Santaquiteria, M., Sánchez-Murcia, P.A., Toro, M.A., de Lucio, H., Gutiérrez, K.J., de Castro, S., Carneiro, F.A.C., Gago, F., Jiménez-Ruiz, A., Camarasa, M.J., Velázquez, S., *Eur J Med Chem.*, **2017**, *135*, 49-59.

[34] Miller, A.F., *Curr. Opin. Chem. Biol.*, **2004**, *8*, 162–168.

[35] Turrens, J.F., *Mol. Asp. Med.* **2004**, *25*, 211–220.